HOCHSCHULE RHEINMAIN

PHYSICS LAB 3

Experiment P3-3
Torsional Pendulum

Authors

HUNTER, DENNIS

KRESS, SEBASTIAN

ÜNLÜ, CIHAN

DEPARTMENT OF ENGINEERING

APPLIED PHYSICS & MEDICAL TECHNOLOGY

Date of experiment: Dezember 15, 2020
Date of submission: January 18, 2021

Contents

1 Introduction

1.1 Terms and Definitions

Free Harmonic and Damped Oscillation

If a system capable of oscillation is deflected out of its equilibrium position and is experiencing a restoring force proportional to its deflection this system is called a *harmonic oscillator*. If a dampening force such as friction is introduced, the system no longer oscillates freely but rather damped.
Both, damped and harmonic oscillations are considered *free* if there is no continuous, the oscillation driving stimulus present.

Natural Angular Frequency of a Harmonic Oscillation

Depending on the very characteristics of the given system it will oscillate at a distinct frequency - the natural angular frequency ω_0.

Differential Equation of the Damped Harmonic Oscillation

$$I\ddot{\varphi} = -D\varphi - \rho\dot{\varphi} + M\cos(\omega t) \tag{1.1}$$

Damping cases

Overdamped: The system returns to equilibrium without oscillating.
Critically damped: The system returns to equilibrium as quickly as possible without oscillating.
Underdamped: The system oscillates (at reduced frequency compared to the undamped case) with the amplitude gradually decreasing to zero.

Rotational Inerta

A cylindrical rot has a rotational inertia about its center of: $I_S = \frac{1}{12}ml^2$

Steiner's Theorem

STEINER's Theorem: $I = I_S + md^2$

Eddy Current Brake

The equivalent circuit of a conductor exposed to a changing magnetic field is composed of only a voltage source and a resistor. The voltage across this resistor is induced as of the law of electromagnetic induction: $U_{ind} = -NA\frac{\partial B}{\partial t}$. The resulting current creates a magnetic field opposing the inducing field. If the change of the inducing magnetic field is due to a mechanical movement, the induced magnetic field will this movement as well.

Constant Current Constant Voltage Operation of a PSU

As the name implies a power supply in CC/CV (**C**onstant **C**urrent/**C**onstant **V**oltage) operation mode keeps the output current and/or output voltage constant independently of the load applied.

Capacitance of a Parallel Plate Capacitor

The capacitance of a parallel plate capacitor is: $C = \varepsilon_0 \varepsilon_r \cdot \frac{A}{d}$

Time-Constant of an RC-Circuit

The time constant of an RC circuit: $\tau = RC$

1.2 Preparation

1.2.1 Deriving the Equation for Damped Free Oscillation

$$\vec{M}_{Inert} + \vec{M}_{Frict} + \vec{M}_{Rest} = 0 \quad \Leftrightarrow \quad J \cdot \ddot{\varphi}(t) - k \cdot \dot{\varphi}(t) - D^* \cdot \varphi(t) = 0 \tag{1.2}$$

can be written as

$$\ddot{\varphi}(t) + 2\delta \cdot \dot{\varphi}(t) + \omega_0^2 \cdot \varphi(t) = 0 \tag{1.3}$$

with

$$-\frac{k}{J} = 2\delta, \quad -\frac{D^*}{J} = \omega_0^2 \tag{1.4}$$

whereas eq. 1.3 is a second degree harmonic differential equation. The chosen approach is:

$$\varphi(t) = \hat{\varphi} e^{\lambda t}, \quad \dot{\varphi}(t) = \lambda \hat{\varphi} e^{\lambda t}, \quad \ddot{\varphi}(t) = \lambda^2 \hat{\varphi} e^{\lambda t} \tag{1.5}$$

Plugged into eq. 1.3 gives

$$\begin{aligned} \left(\lambda^2 + 2\delta\lambda + \omega_0^2\right) \hat{\varphi} e^{\lambda t} &= 0 \\ \lambda_{1,2} &= -\delta \pm \sqrt{\delta^2 - \omega_0^2} \end{aligned} \tag{1.6}$$

Here two possible cases are to be distinguished:

$$\lambda_{1,2} = \begin{cases} -\delta \pm i\omega_d & \text{for} \quad \delta^2 < \omega_0^2 \quad \text{(a)} \\ -\delta \pm \omega_d & \text{for} \quad \delta^2 \geq \omega_0^2 \quad \text{(b)} \end{cases} \tag{1.7}$$

In eq. 1.3:

$$\varphi_1(t) = \varphi_1 e^{-\delta + i\omega_d t}, \quad \varphi_2(t) = \varphi_2 e^{-\delta - i\omega_d t} \tag{1.8}$$

Linear combination of $\varphi_1(t)$ and $\varphi_2(t)$ lastly leads to

$$\varphi(t) = \varphi_1 e^{-\delta + i\omega_d t} + \varphi_2 e^{-\delta - i\omega_d t} = \hat{\varphi} e^{-\delta t} \cdot \cos\left(\omega_d t + \varphi_0\right) \tag{1.9}$$

1.2.2 Damping Cases

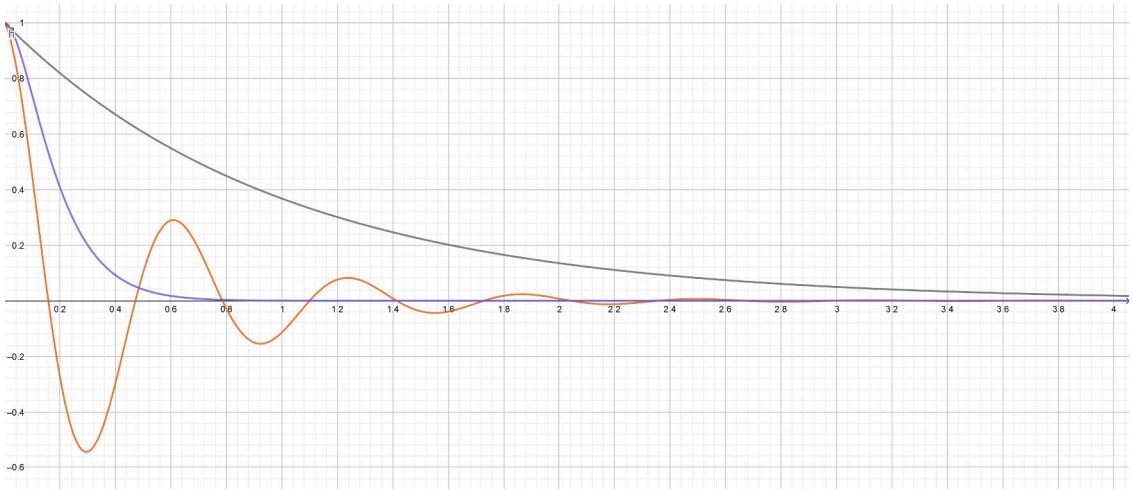

Figure 1.1: Plot of amplitude against time of a harmonic oscillation with parameterized damping coefficient. Orange: underdamped, Gray: overdamped, Blue: critically damped.

1.2.3 Unknown Angular Inertia of the Pendulum

The angular inertia of the pendulum J_P can be determined by adding a known angular inertia J_R of a cylindrical rod. As eq. 1.4 delivers

$$\omega_0 = \sqrt{\frac{D^*}{J}} \tag{1.10}$$

and $\omega = \frac{2\pi}{T}$, the following relation is given:

$$\omega_{0,P} = \sqrt{\frac{D^*}{J_P}} = \frac{2\pi}{T_P} \quad \Leftrightarrow \quad 2\pi = T_P \cdot \sqrt{\frac{D^*}{J_P}} \tag{1.11}$$

$$\omega_{0,P+R} = \sqrt{\frac{D^*}{J_P + J_R}} = \frac{2\pi}{T_{P+R}} \quad \Leftrightarrow \quad 2\pi = T_{P+R} \cdot \sqrt{\frac{D^*}{J_P + J_R}} \tag{1.12}$$

When eq. 1.11 and eq. 1.12 are equated:

$$\begin{aligned} & T_P \cdot \sqrt{\frac{D^*}{J_P}} = T_{P+R} \cdot \sqrt{\frac{D^*}{J_P + J_R}} \\ \Leftrightarrow \quad & \left(\frac{T_{P+R}}{T_P}\right)^2 = \frac{J_P + J_R}{J_P} = 1 + \frac{J_R}{J_P} \\ \Leftrightarrow \quad & \frac{J_R}{J_P} = \left(\frac{T_{P+R}}{T_P}\right)^2 - 1 \\ \Rightarrow \quad & J_P = \frac{J_R}{\left(\frac{T_{P+R}}{T_P}\right)^2 - 1} \end{aligned} \tag{1.13}$$

The angular inertia of the pendulum can be calculated without knowing the torsion constant D^*.

1.2.4 Rotational Inertia of a Cylindrical Rod

Inertia of a rotating mass dimensionless mass is proportional to the square of the distance to its rotational axis. As the mass of a cylindrical body is distributed over its volume, it is necessary to integrate over all dm along the distance r from the center of rotation. [1]

$$J_Z = \int r^2 dm \tag{1.14}$$

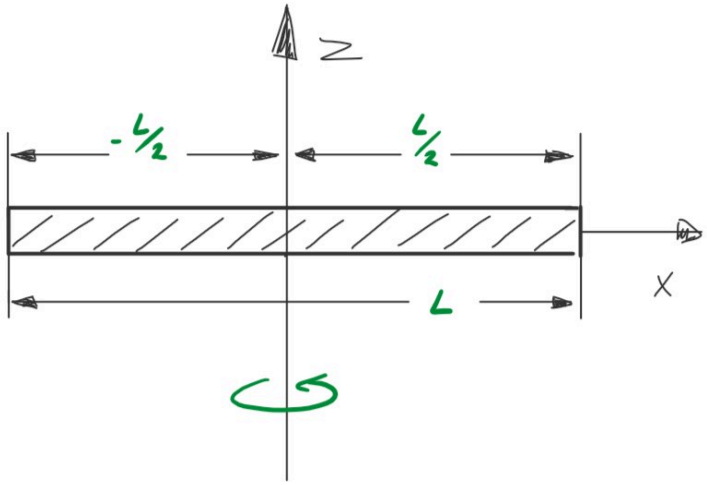

Figure 1.2: Scheme of an orthogonally to its center axis rotating rod.

With

$$\rho = \frac{dm}{dx} = \frac{M}{L} \qquad \Leftrightarrow \qquad dm = \frac{M}{L}dx \tag{1.15}$$

plugged into eq. 1.14 with respect to the integration limits as of fig. 1.2 gives

$$J_Z = \int_{-L/2}^{L/2} \frac{M}{L}x^2 dx = \frac{1}{12}ML^2 \tag{1.16}$$

1.2.5 Equations for the Sensor Capacitances

To derive:

$$C_1(\varphi) = \varepsilon_0 \frac{\pi D^2}{16d}\left(1 - \frac{2\varphi}{\pi}\right) \tag{1.17}$$

$$C_2(\varphi) = \varepsilon_0 \frac{\pi D^2}{16d}\left(1 + \frac{2\varphi}{\pi}\right) \tag{1.18}$$

with

$$A_{1,2}(\varphi) = \frac{1}{16}\pi D^2\left(1 \pm \frac{2\varphi}{\pi}\right) \tag{1.19}$$

One half of the stator pairs together with the rotor plate forms two capacitors connected in series. With each capacitor having the same value at any time the total capacitance equates to

$$C_{1,2}(\varphi) = \varepsilon_0 \varepsilon_r \frac{A(\pm\varphi)}{2d} \tag{1.20}$$

Where $A(\varphi)$ can be expressed as

$$\begin{aligned} A(\varphi) &= \frac{1}{8}D^2(\pi \pm \varphi) \\ A(\varphi) &= \frac{1}{8}D^2\left(\frac{\pi^2}{\pi} \pm \frac{\pi\varphi}{\pi}\right) \\ A(\varphi) &= \frac{1}{8}\pi D^2\left(1 \pm \frac{\varphi}{\pi}\right) \end{aligned} \tag{1.21}$$

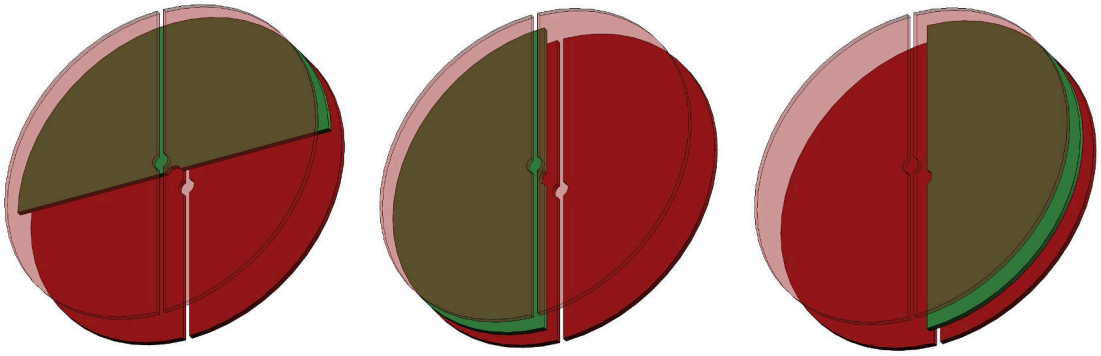

(a) Rotor at $\varphi = 0$ *(b)* Rotor at $\varphi = \pm\frac{\pi}{2}$ *(c)* Rotor at $\varphi = \mp\frac{\pi}{2}$

Figure 1.3: Schematical assembly of the angular sensor. The semi circular rotor plate (green) sandwiched between the two stators (red). The area of the rotor facing one of the vertical stator pairs varies with the angular displacement φ of the rotor.

Say the zero position is chosen such as the whole area of the rotor takes effect (see fig. 1.3c) eq. 1.21 maximizes. Thus, the absolute capacitance of one of the capacitors is maximized. Stepping the rotor about $\varphi = \frac{\pi}{2}$ as seen in fig. 1.3a halves the effective area of the capacitor halving the total capacitance. At an angular displacement of $\varphi = \pi$ the capacitance equates to zero respectively.
Combining eq. 1.20 and eq. 1.21 gives [1]

$$C_{1,2} = \varepsilon_0 \frac{\pi D^2}{16d} \left(1 \pm \frac{2\varphi}{\pi}\right) \tag{1.22}$$

$$\left(1 \pm \frac{2\varphi}{\pi}\right) \begin{cases} = 0 & \text{for} \quad \varphi = \pm\frac{\pi}{2} \\ = 1 & \text{for} \quad \varphi = 0 \\ = 2 & \text{for} \quad \varphi = \mp\frac{\pi}{2} \end{cases}$$

1.2.6 Time to Reach the Threshold Voltage

The charging curve of a capacitor is given by eq. 1.23.

$$U_C(t) = U_0 \left(1 - exp\left(-\frac{t}{\tau}\right)\right) \tag{1.23}$$

Being interested at the time t_{th} it takes to reach a certain threshold voltage U_{th}, eq. 1.23 can be transformed as follows:

$$1 - \frac{U_{th}}{U_0} = exp\left(-\frac{t_{th}}{\tau}\right)$$

$$\Leftrightarrow$$

$$t_{th} = -\ln\left(1 - \frac{U_{th}}{U_0}\right) \cdot \tau \tag{1.24}$$

with the time constant $\tau = R \cdot C$.

1.2.7 Determining the Angular Deflection by the Difference of Timer Ticks

The time to reach the threshold voltage as of eq. 1.24 is captured independently due to each capacitor being connected to individual GPIOs.

[1] The solution is missing a factor of 2 in front of φ

Since the charging curve of the capacitors differs in an anti-proportional manner when an angular deflection takes place the absolute value of the time difference gives the angle about zero while the sign gives the direction. Therefore, taken these considerations in account and merging eq. 1.20 and eq. 1.24 gives:

$$\begin{aligned}\Delta t_{th}(\varphi) &= t_{th,1} - t_{th,2} = -\ln\left(1-\frac{U_{th}}{U_0}\right) R\left[C_1(\varphi) - C_2(\varphi)\right] \\ &= -\varepsilon_0 R \frac{\pi D^2}{16d} \ln\left(1-\frac{U_{th}}{U_0}\right)\left[\left(1+\frac{2\varphi}{\pi}\right) - \left(1-\frac{2\varphi}{\pi}\right)\right] \\ &= -\varepsilon_0 R \frac{4D^2}{16d} \ln\left(1-\frac{U_{th}}{U_0}\right) \cdot \varphi \end{aligned} \tag{1.25}$$

Here ε_0, R, D, d, U_{th} and U_0 remain constant and can be gathered as a proportionality factor. This reduces eq. 1.25 to

$$\Delta t_{th}(\varphi) = \chi \cdot \varphi \tag{1.26}$$

The µC checks the state of the input pin once every cycle. To take that into account the difference in threshold time Δt_{th} has to be divided by the cycle time Δt of the µC which gives the number of cycles it took for the input pins to switch state from low to high. If a change takes place at a non integer multiple of Δt the µC will register a transition on the subsequent cycle, thus, for the cycle count n applies $n \in \mathbb{N}$. Furthermore, a non-integer value for n has to be rounded up to the next integer value.
Mathematically the above considerations yield

$$n(\varphi) = \left\lceil \frac{|\Delta t_{th}(\varphi)|}{\Delta t} \right\rceil = \lceil \chi' \cdot |\varphi| \rceil \qquad \text{with} \qquad n(\varphi) : n(\varphi) \in \mathbb{N} \tag{1.27}$$

which translates into the amount of deflection and

$$\frac{|n(\varphi)|}{n(\varphi)} = \pm 1 \tag{1.28}$$

to distinguish between a CW/CCW rotation.

1.2.8 Sensitivity of the Angular Sensor

As seen in eq. 1.26 the tick rate relates linearly with the angular displacement φ. Therefore, the maximum resolution of the angular sensor expressed as *ticks per radiant* **is** χ'.

$$\frac{dn(\varphi)}{d\varphi} = \chi' \cdot \varphi \frac{d}{d\varphi} = \chi' \tag{1.29}$$

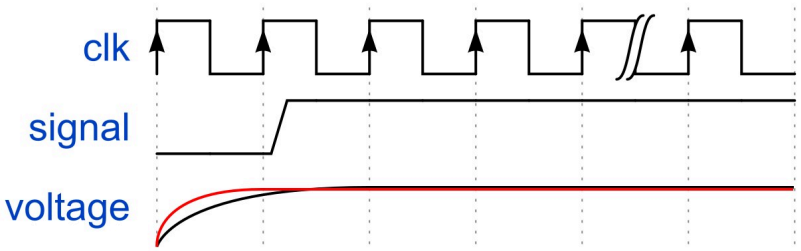

Figure 1.4: Timing diagram showing the signal transition.

The clock frequency of the µC is $f = 16\,\text{MHz}$ which gives a cycle time of $\delta t = 62.5\,\text{ns}$.

To ready the capacitors for the next charging cycle they need to be discharged as quick as possible. Considering that a time to discharge the capacitors $< \Delta t$ makes no significant difference the unknown value R of the resistor can be approximated as

$$\begin{aligned} 3\tau = \Delta t &= 3RC \\ &\Leftrightarrow \\ \frac{\Delta t}{3C_{max}} &= R \end{aligned} \tag{1.30}$$

In the equation above the assumptions are made that a discharge rate of 95% is sufficient and the circuit needs to be able to discharge the capacitor within the timeframe Δt while being at its maximum capacitance. Thus,

$$\begin{aligned} C_{max} &= \varepsilon_0 \frac{\pi D^2}{8d} \\ &= 8,85 \cdot 10^{-12} \frac{\mathrm{As}}{\mathrm{Vm}} \frac{\pi \cdot 0.12^2\,\mathrm{m}^2}{8 \cdot 0.01\,\mathrm{m}} \\ &= 5.01\,\mathrm{pF} \end{aligned} \tag{1.31}$$

in eq. 1.30 gives a value for the resistance as

$$\frac{62.5\,\mathrm{ns}}{3 \cdot 5.01\,\mathrm{pF}} \approx 4160.9\,\mathrm{k\Omega} \tag{1.32}$$

This lies between the two more common E-Series values of $4.7\,\mathrm{k\Omega}$ and $3.9\,\mathrm{k\Omega}$. For further calculations the latter is chosen as a higher resistance would increase the discharge time.

Plugging in the given values of for $\varepsilon_0, D, d, U_{th}, U_0$ and the calculated values for Δt and R equates eq. 1.26 to

$$\begin{aligned} \chi' &= -\varepsilon_0 R \frac{4D^2}{16d} \ln\left(1 - \frac{U_{th}}{U_0}\right) \Delta t^{-1} \\ &= -8.85 \cdot 10^{-12} \frac{\mathrm{As}}{\mathrm{Vm}} \cdot 3.9\,\mathrm{k\Omega} \cdot \frac{4 \cdot 0.12^2\,\mathrm{m}^2}{16 \cdot 0.01\,\mathrm{m}} \ln\left(1 - \frac{2.5\,\mathrm{V}}{5\,\mathrm{V}}\right) \cdot \frac{1}{62.5\,\mathrm{ns}} \\ &\approx 0.138\,\mathrm{rad}^{-1} \end{aligned} \tag{1.33}$$

2 Set-Up of Experiment

The equipment and materials that are needed to perform the experiments are shown in fig. 2.1. A detailed view of the angular sensor assembly is seen in fig. 2.2.
Using a desktop computer a serial connection via USB to the µC board is established. A serial monitor - REALTERM - is used to log the inbound stream send by the µC. The relevant settings are listed below:

- 9600 Baud
- On the `Display` tab, `Ascii` and `new Line mode` are checked, `Direct capture` remains un-checked.
- COM-Port as assigned by the OS.

The data is now continuously sent by the µC. The data is displayed on the screen. A text file is created in which the data is written and saved. Two columns are displayed. The first column contains the time t in seconds, the second the number of timer ticks n. The current source for the electromagnet is switched on. Now the setup is completed and the experiments can be started.

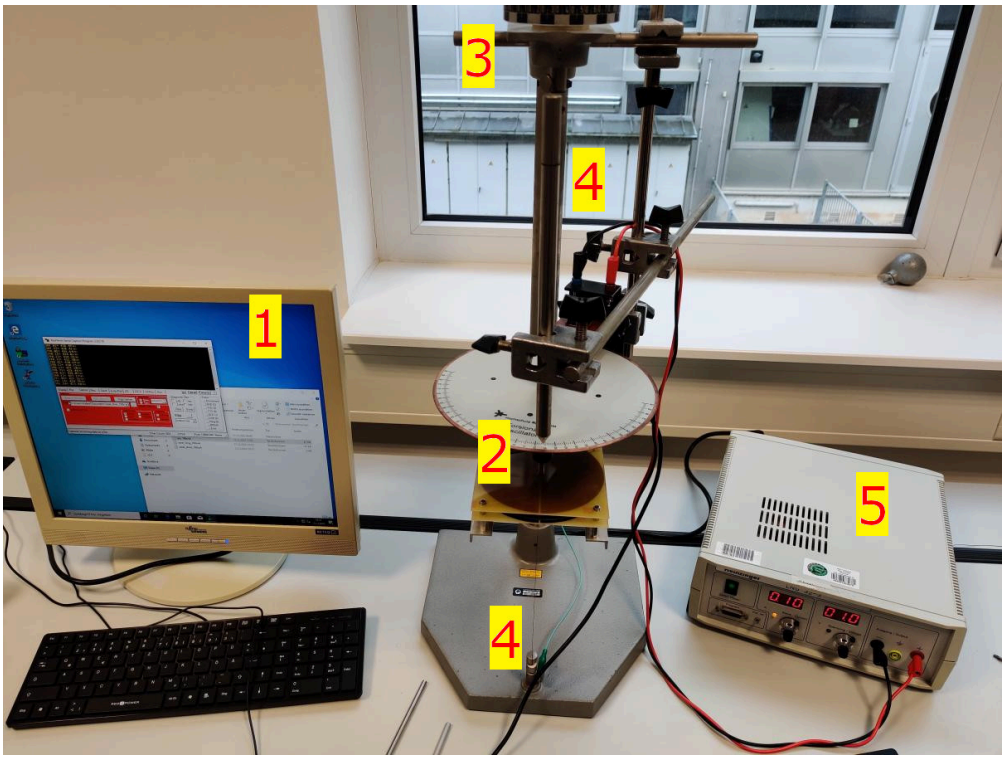

Figure 2.1: Equipment and material required for the experiments. 1. Computer running REALTERM, 2. Angular sensor assembly, 3. Zero adjustment, 4. Torsion wire, 5. PSU in constant current mode powering the eddy current brake.

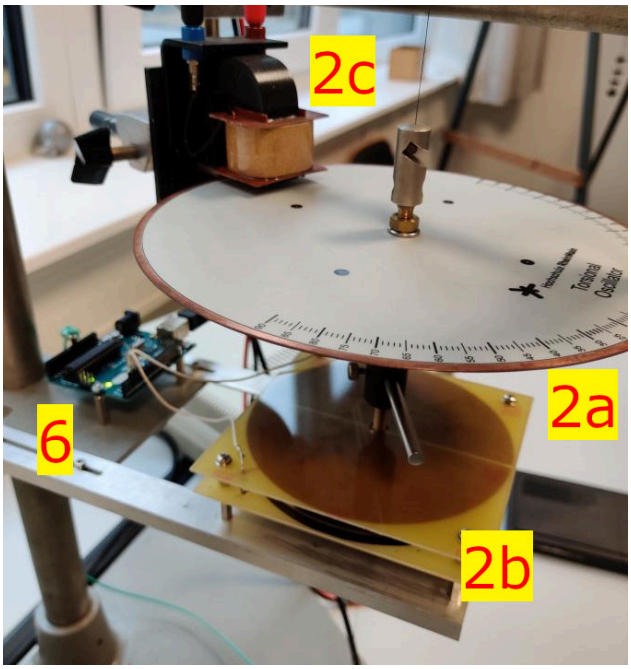

Figure 2.2: Detailed view of the angular sensor assembly. 2a: Copper plate with scale in degree, 2b: Capacitor plates, 2c: Eddy current brake, 6: µC board.

3 Execution

3.1 Angular Sensor

The current through the electromagnet, which operates the eddy current brake, is set to $I = 1\,\mathrm{A}$. With the zero adjustment (No. 3 in fig. 2.1), the copper disk is set to a deflection of $\varphi = -90°$. The recording using REALTERM is started. Some values are captured and saved. The deflection is decreased by 10° and a new recording is started and saved. This process is repeated in increments of 10° until a deflection of $\varphi = +90°$ is reached. At the end, the current through the electromagnet is set back to $I = 0\,\mathrm{A}$.

3.2 Torsional Pendulum

3.2.1 Natural Angular Frequency and Damping Coefficient

The deflection of the pendulum is set back to $\varphi = 0°$ by zero adjustment. Seven series of measurements are recorded and saved. Each measurement series runs for 300 s. Each time a different current is set, as shown in table 3.1. At each measurement, the disk is carefully deflected to $\varphi = 75°$ and held. At the moment the reset button on the microcontroller is pressed, the pendulum is released while avoiding unnecessary oscillations. At higher currents, the oscillation ends before the completion of the 300 s. In these cases, the capturing is ended earlier.

Table 3.1: Currents set in each measurement.

no.	I
1	0 A
2	0.1 A
3	0.2 A
4	0.3 A
5	0.4 A
6	0.5 A
7	1.3 A

At the end, the current through the electromagnet is set back to $I = 0\,\mathrm{A}$.

3.2.2 Rotational Inertia

The diameter, length, and mass of the three given rods are measured and the values, including their uncertainty, are noted. For this purpose, a measuring caliper, a steel ruler and the balance provided in the laboratory rooms are used. The current is set to $I = 100\,\mathrm{mA}$. The first rod is inserted into the cross bore and carefully screwed tight. The hole is located between the copper plate and the angular sensor. An already mounted rod is shown in fig. 2.2. When mounting, the rod is positioned as centrally as possible in the socket. The disk is carefully deflected to $\varphi = 75°$ and held. At the moment the reset button on the microcontroller is pressed, the pendulum is released avoiding unnecessary oscillations. The measurement ends after the pendulum has come to rest. The data is saved and the measurement is repeated for the other rods.

4 Evaluation

4.1 Angular Sensor

Before investigating the dependence of the angle and the timer ticks, it is needed to determine the mean value of the timer ticks for each angle. The mean values are computed taking 20 samples each.

Table 4.1: Mean value of timer ticks per angular displacement

$\varphi/^\circ$	$\bar{n}$	$\varphi/^\circ$	$\bar{n}$
$+90$	601.34	-10	-55.33
$+80$	549.63	-20	-126.04
$+70$	482.26	-30	-195.80
$+60$	421.93	-40	-262.31
$+50$	353.10	-50	-331.20
$+40$	288.13	-60	-396.87
$+30$	220.58	-70	-459.46
$+20$	147.85	-80	-474.44
$+10$	83.57	-90	-499.79
$+0$	14.36		

In fig. 4.1 the timer ticks n are plotted as a function of the angle φ.

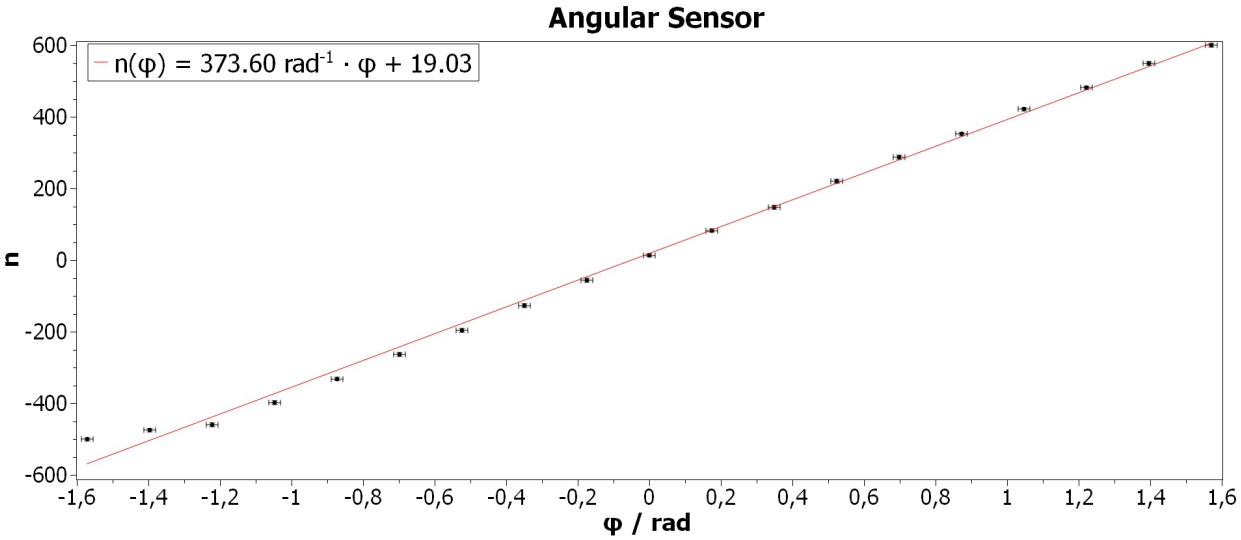

Figure 4.1: Curve of the angular sensor

The sensitivity corresponds to the slope of the curve and the offset to the intercept.
The computed fit is

$$n(\varphi) = 373.60\,\mathrm{rad}^{-1} \cdot \varphi + 19.03 \tag{4.1}$$

which gives values for the sensitivity s and the offset o of

$$s = 374\,\mathrm{rad}^{-1} \pm 1\,\mathrm{rad}^{-1} \tag{4.2}$$

$$o = 19 \pm 1 \tag{4.3}$$

Cihans Comparison

4.2 Torsional Pendulum

4.2.1 Natural Angular Frequency And Damping Coefficient

Figure 4.2 shows the oscillation with a coil current of 100 mA. The respective plots for coil currents ranging from $200 - 500$ mA and the coil current turned off can be seen in fig. A.0. Deflection is plotted versus time. The period time for each curve is determined by reading a few values and building the mean.

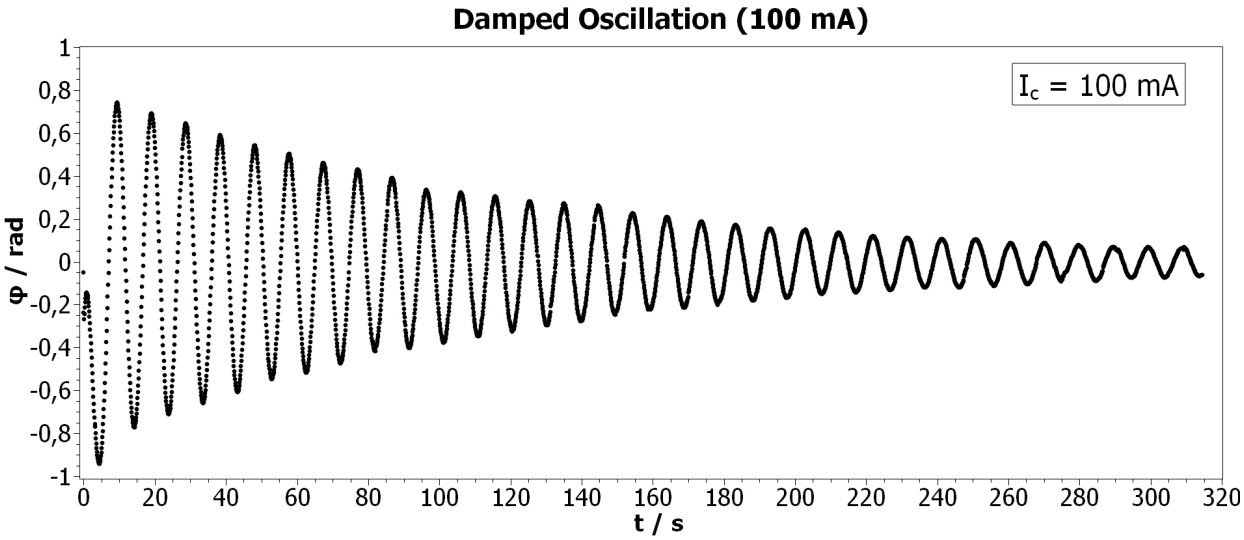

Figure 4.2: Plot of the tick rate over time with a coil current of 100 mA.

The values are as follows:

Table 4.2

T_0	$9.7\,\mathrm{s} \pm 0.5\,\mathrm{s}$	T_{300}	$9.8\,\mathrm{s} \pm 0.5\,\mathrm{s}$
T_{100}	$9.6\,\mathrm{s} \pm 0.5\,\mathrm{s}$	T_{400}	$10.0\,\mathrm{s} \pm 0.5\,\mathrm{s}$
T_{200}	$9.6\,\mathrm{s} \pm 0.5\,\mathrm{s}$	T_{500}	$10.4\,\mathrm{s} \pm 0.5\,\mathrm{s}$

Thus, the damped natural frequencies are calculated using $\omega = \frac{2\pi}{T}$:

Table 4.3

$\omega_{d,0}$	$0.65\,\mathrm{s}^{-1} \pm 0.03\,\mathrm{s}^{-1}$	$\omega_{d,300}$	$0.64\,\mathrm{s}^{-1} \pm 0.03\,\mathrm{s}^{-1}$
$\omega_{d,100}$	$0.65\,\mathrm{s}^{-1} \pm 0.03\,\mathrm{s}^{-1}$	$\omega_{d,400}$	$0.63\,\mathrm{s}^{-1} \pm 0.03\,\mathrm{s}^{-1}$
$\omega_{d,200}$	$0.64\,\mathrm{s}^{-1} \pm 0.03\,\mathrm{s}^{-1}$	$\omega_{d,500}$	$0.60\,\mathrm{s}^{-1} \pm 0.03\,\mathrm{s}^{-1}$

The deviations of the period time are reading errors. The ones of the damped natural frequency can be calculated with

$$\begin{aligned}\Delta\omega_d &= \left|\frac{\partial\omega_d}{\partial T}\right| \cdot \Delta T \\ &= \frac{2\pi}{T^2} \cdot \Delta T \end{aligned} \tag{4.4}$$

for $\omega_{d,0}$ e.g.:

$$\begin{aligned}\Delta\omega_{d,0} &= \frac{2\pi}{(9.7\,\mathrm{s})^2} \cdot 0.5\,\mathrm{s} \\ &= 0.03\,\mathrm{s}^{-1} \end{aligned} \tag{4.5}$$

The damping coefficient can be determined by way of

$$\begin{aligned}\varphi_1 \cdot e^{-\delta t_0} &= \varphi_0 \cdot e^{-\delta t_1} \\ e^{\delta(t_1-t_0)} &= \frac{\varphi_0}{\varphi_1} \\ \delta(t_1-t_0) &= \ln\frac{\varphi_0}{\varphi_1} \\ \delta &= (t_1-t_0)^{-1} \cdot \ln\frac{\varphi_0}{\varphi_1} \end{aligned} \tag{4.6}$$

The times and angles have been read and δ has been calculated individually.
This gives us the following mean values:

Table 4.4

δ_0	$0.002\,\mathrm{s}^{-1} \pm 0.001\,\mathrm{s}^{-1}$	δ_{300}	$0.08\,\mathrm{s}^{-1} \pm 0.01\,\mathrm{s}^{-1}$
δ_{100}	$0.008\,\mathrm{s}^{-1} \pm 0.002\,\mathrm{s}^{-1}$	δ_{400}	$0.12\,\mathrm{s}^{-1} \pm 0.01\,\mathrm{s}^{-1}$
δ_{200}	$0.03\,\mathrm{s}^{-1} \pm 0.01\,\mathrm{s}^{-1}$	δ_{500}	$0.22\,\mathrm{s}^{-1} \pm 0.01\,\mathrm{s}^{-1}$

For the deviation, the standard deviation is used. Otherwise, it can also be determined by means of the partial derivation:

$$\begin{aligned}\Delta\delta &= \left|\frac{\partial\delta}{\partial t_1}\right| \cdot \Delta t_1 + \left|\frac{\partial\delta}{\partial t_0}\right| \cdot \Delta t_0 + \left|\frac{\partial\delta}{\partial\varphi_0}\right| \cdot \Delta\varphi_0 + \left|\frac{\partial\delta}{\partial\varphi_1}\right| \cdot \Delta\varphi_1 \\ &= \frac{1}{(t_1-t_0)^2} \cdot \ln\frac{\varphi_0}{\varphi_1} \cdot (\Delta t_0 + \Delta t_1) + \frac{1}{(t_1-t_0)} \cdot \left(\frac{1}{\varphi_0} \cdot \Delta\varphi_0 + \frac{1}{\varphi_1} \cdot \Delta\varphi_1\right) \end{aligned} \tag{4.7}$$

The natural angular frequencies are calculated via $\omega_0 = \sqrt{\omega_d^2 + \delta^2}$ as

Table 4.5

$\omega_{0,0}$	$0.65\,\mathrm{s}^{-1} \pm 0.03\,\mathrm{s}^{-1}$	$\omega_{0,300}$	$0.65\,\mathrm{s}^{-1} \pm 0.03\,\mathrm{s}^{-1}$
$\omega_{0,100}$	$0.65\,\mathrm{s}^{-1} \pm 0.03\,\mathrm{s}^{-1}$	$\omega_{0,400}$	$0.64\,\mathrm{s}^{-1} \pm 0.03\,\mathrm{s}^{-1}$
$\omega_{0,200}$	$0.64\,\mathrm{s}^{-1} \pm 0.03\,\mathrm{s}^{-1}$	$\omega_{0,500}$	$0.68\,\mathrm{s}^{-1} \pm 0.03\,\mathrm{s}^{-1}$

and their deviations via

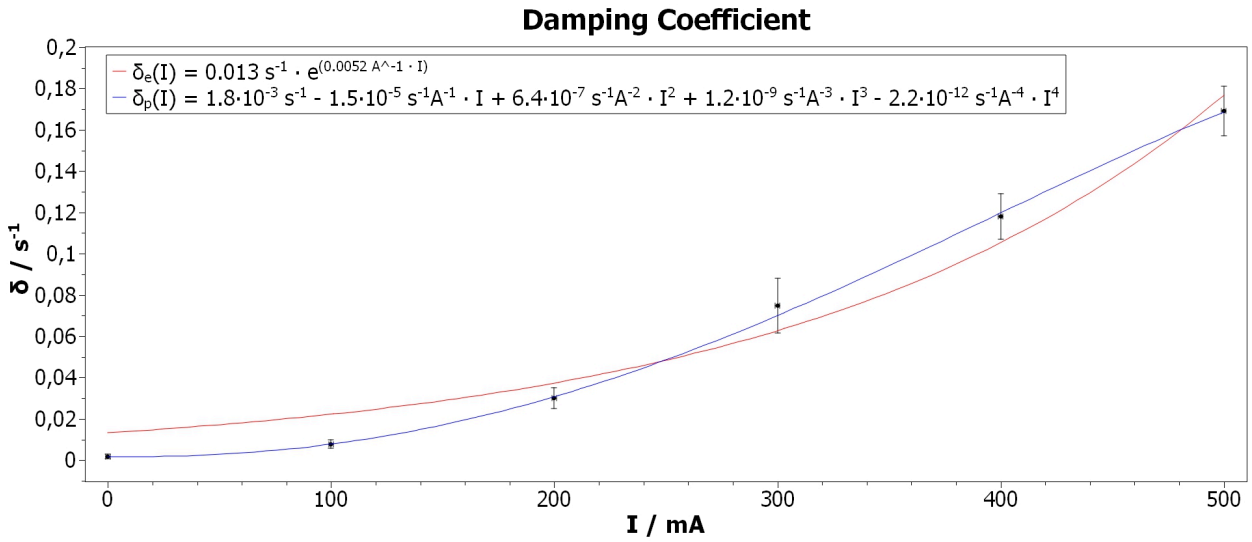

Figure 4.3: Damping coefficient depending on the coil current

$$\begin{aligned}\Delta\omega_0 &= \left|\frac{\partial\omega_0}{\partial\omega_d}\right|\cdot\Delta\omega_0 + \left|\frac{\partial\omega_0}{\partial\delta}\right|\cdot\Delta\delta \\ &= \frac{\omega_d}{\sqrt{\omega_d^2+\delta^2}}\cdot\Delta\omega_d + \frac{\delta}{\sqrt{\omega_d^2+\delta^2}}\cdot\Delta\delta \end{aligned} \tag{4.8}$$

for $\omega_{0,0}$ e.g. as

$$\begin{aligned}\Delta\omega_{0,0} &= \frac{0.65\,\mathrm{s}^{-1}}{\sqrt{0.65\,\mathrm{s}^{-1}+0.002\,\mathrm{s}^{-1}}}\cdot 0.03\,\mathrm{s}^{-1} + \frac{0.002\,\mathrm{s}^{-1}}{\sqrt{0.65\,\mathrm{s}^{-1}+0.002\,\mathrm{s}^{-1}}}\cdot 0.001\,\mathrm{s}^{-1} \\ &= 0.03\,\mathrm{s}^{-1} + 3\cdot 10^{-6}\mathrm{s}^{-1} \\ &\approx 0.03\,\mathrm{s}^{-1}\end{aligned}$$

In fig. 4.3 the damping coefficient is plotted versus coil current. For finding a formula $\delta(I)$ SciDAVis did an exponential fit $\delta_e(I)$ (red curve) and a fourth degree polynomial fit $\delta_p(I)$ (blue curve):

$$\delta_e(I) = 0.013\,\mathrm{s}^{-1}\cdot e^{0.0052\,\mathrm{A}^{-1}\cdot I} \tag{4.9}$$

$$\begin{aligned}\delta_p(I) =& 1.8\cdot 10^{-3}\mathrm{s}^{-1} - 1.5\cdot 10^{-5}\mathrm{s}^{-1}\mathrm{A}^{-1}\cdot I + 6.4\cdot 10^{-7}\mathrm{s}^{-1}\mathrm{A}^{-2}\cdot I^2 \\ &+ 1.2\cdot 10^{-9}\mathrm{s}^{-1}\mathrm{A}^{-3}\cdot I^3 + 2.2\cdot 10^{-12}\mathrm{s}^{-1}\mathrm{A}^{-4}\cdot I^4\end{aligned} \tag{4.10}$$

As it can be seen, the polynomial fit is a better approximation than the exponential. However, the polynomial curve is only a good approach in the area of $0 \leq I \leq 500\,\mathrm{mA}$. At higher currents the curve has a maximum and goes lower again, which is illogical in the physical sense. Therefore, the exponential curve is a qualitatively better description of the dependency.

Finally, the aperiodic case is considered and plotted in fig. 4.4.

4.2.2 Rotational Inertia

To determine the unknown rotational inertia of the pendulum, the dimensions of each of the three rods must first be measured as it can be seen in table 4.6.

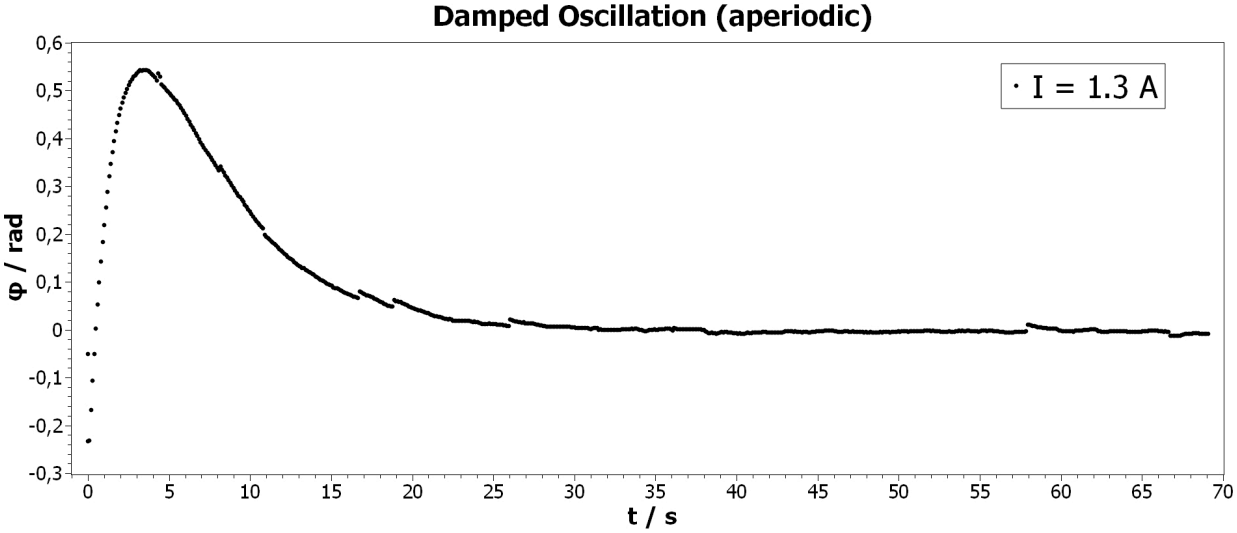

Figure 4.4: Aperiodic damped oscillation at $I_c = 1.3\,\mathrm{A}$

Table 4.6: rod dimensions

i	$m_{Ri}/\,\mathrm{g}$	$D_{Ri}/\,\mathrm{mm}$	$l_{Ri}/\,\mathrm{mm}$
1	8.89 ± 0.01	5.95 ± 0.05	120 ± 0.05
2	26.73 ± 0.01	6.00 ± 0.05	120 ± 0.05
3	56.38 ± 0.01	6.00 ± 0.05	240 ± 0.5

Obviously, the diameters all are much smaller than the lengths. Hence, the rotational rod inertia can be calculated by means of eq. 1.16.
The following values are obtained:

$$J_{R1} = 10670\,\mathrm{g}\cdot\mathrm{mm}^2 \pm 21\,\mathrm{g}\cdot\mathrm{mm}^2 \tag{4.11}$$
$$J_{R2} = 32080\,\mathrm{g}\cdot\mathrm{mm}^2 \pm 39\,\mathrm{g}\cdot\mathrm{mm}^2 \tag{4.12}$$
$$J_{R3} = 270600\,\mathrm{g}\cdot\mathrm{mm}^2 \pm 1200\,\mathrm{g}\cdot\mathrm{mm}^2 \tag{4.13}$$

The deviations of the rod dimensions are reading errors of the scales. The deviations of the rod inertia can be determined by way of:

$$\begin{aligned}\Delta J_{Ri} &= \left|\frac{\partial J_{Ri}}{\partial m_{Ri}}\right| \cdot \Delta m_{Ri} + \left|\frac{\partial J_{Ri}}{\partial l_{Ri}}\right| \cdot \Delta l_{Ri} \\ &= \frac{1}{12} \cdot l_{Ri}^2 \cdot \Delta m_{Ri} + \frac{1}{6} \cdot m_{Ri} \cdot l_{Ri} \cdot \Delta l_{Ri}\end{aligned} \tag{4.14}$$

For J_{R2} it is e.g.:

$$\begin{aligned}\Delta J_{R2} &= \frac{1}{12} \cdot (120\,\mathrm{mm})^2 \cdot 0.01\,\mathrm{g} + \frac{1}{6} \cdot 26.73\,\mathrm{g} \cdot 120\,\mathrm{mm} \cdot 0.05\,\mathrm{mm} \\ &= 12\,\mathrm{g}\cdot\mathrm{mm}^2 + 26.73\,\mathrm{g}\cdot\mathrm{mm}^2 \\ &= 38.73\,\mathrm{g}\cdot\mathrm{mm}^2 \approx 39\,\mathrm{g}\cdot\mathrm{mm}^2\end{aligned}$$

The mean values of the period times read with reading errors are as follows:

$$T_{P+R1} = 9.7\,\mathrm{s} \pm 0.3\,\mathrm{s} \tag{4.15}$$
$$T_{P+R2} = 9.8\,\mathrm{s} \pm 0.3\,\mathrm{s} \tag{4.16}$$
$$T_{P+R3} = 11.3\,\mathrm{s} \pm 0.3\,\mathrm{s} \tag{4.17}$$
$$T_P = 9.7\,\mathrm{s} \pm 0.3\,\mathrm{s} \qquad \text{(without rod)} \tag{4.18}$$

With eq. 1.13 the unknown pendulum inertia are calculated as:

$$J_{P1} = (\text{error}) \tag{4.19}$$
$$J_{P2} = 1286000\,\mathrm{g \cdot mm^2} \pm 6000\,\mathrm{g \cdot mm^2} \tag{4.20}$$
$$J_{P3} = 760000\,\mathrm{g \cdot mm^2} \pm 34000\,\mathrm{g \cdot mm^2} \tag{4.21}$$

The uncertainties are determined as follows:

$$\begin{aligned}
\Delta J_P &= \left|\frac{\partial J_P}{\partial J_R}\right| \cdot \Delta J_R + \left|\frac{\partial J_P}{\partial T_{P+R}}\right| \cdot \Delta T_{P+R} + \left|\frac{\partial J_P}{\partial T_P}\right| \cdot \Delta T_P \\
&= \frac{1}{\left(\frac{T_{P+R}}{T_P}\right)^2 - 1} \cdot \Delta J_R + \frac{2 \cdot J_R \cdot T_{P+R}}{T_P^2 \cdot \left(\frac{T_{P+R}^2}{T_P^2} + 1\right)} \cdot \Delta T_{P+R} + \frac{2 \cdot J_R \cdot T_{P+R}^2}{T_P^3 \cdot \left(\frac{T_{P+R}^2}{T_P^2} + 1\right)} \cdot \Delta T_P \qquad \Big| \Delta T_{P+R} = \Delta T_P \\
&= \frac{1}{\left(\frac{T_{P+R}}{T_P}\right)^2 - 1} \cdot \Delta J_R + \left(\frac{2 \cdot J_R \cdot T_{P+R}}{T_P^2 \cdot \left(\frac{T_{P+R}^2}{T_P^2} + 1\right)} + \frac{2 \cdot J_R \cdot T_{P+R}^2}{T_P^3 \cdot \left(\frac{T_{P+R}^2}{T_P^2} + 1\right)} \right) \cdot \Delta T_P
\end{aligned} \tag{4.22}$$

For J_{P3} it results:

$$\begin{aligned}
\Delta J_{P3} &= \frac{1}{\left(\frac{11.3\,\mathrm{s}}{9.7\,\mathrm{s}}\right)^2 - 1} \cdot 1200\,\mathrm{g \cdot mm^2} + \left(\frac{2 \cdot 270600\,\mathrm{g \cdot mm^2} \cdot 11.3\,\mathrm{s}}{(9.7\,\mathrm{s})^2 \cdot \left(\frac{(11.3\,\mathrm{s})^2}{(9.7\,\mathrm{s})^2} + 1\right)} + \frac{2 \cdot 270600\,\mathrm{g \cdot mm^2} \cdot (11.3\,\mathrm{s})^2}{(9.7\,\mathrm{s})^3 \cdot \left(\frac{(11.3\,\mathrm{s})^2}{(9.7\,\mathrm{s})^2} + 1\right)} \right) \cdot 0.3\,\mathrm{s} \\
&= 3360\,\mathrm{g \cdot mm^2} + 30981\,\mathrm{g \cdot mm^2} \\
&= 34341\,\mathrm{g \cdot mm^2} \approx 34000\,\mathrm{g \cdot mm^2}
\end{aligned}$$

The calculable values for the pendulum inertia are around $10^6\,\mathrm{g \cdot mm^2}$. The short aluminum rod gives no value for the pendulum inertia, since it shows no noticeable differences in period time. So it seems that the aluminum rod does not change the inertia of the pendulum at all. Furthermore, the two values obtained have relatively large deviations from one another. It is probably due to the avoidable but also less avoidable measurement errors. The latter are external influences, e.g. the vibration of the pendulum caused by table tremors or shaking hands when deflecting the pendulum. On the other hand, reading the period time could be more accurate. As it can be seen in the calculation of the uncertainties, the period time deviation is more perceptible than the rod inertia deviation.

5 Conclusion

In retrospect, the purpose of the experiment can be considered cautiously as achieved. Although there were some problems, the properties of a torsional pendulum were successfully investigated. Initially, the characteristic curve recording of the sensor worked well, thus confirming the functionality of the capacitor. Unfortunately, from the determination of the damped vibration, a few problems occurred with the program REALTERM and the µC. The timer ticks no longer corresponded to the angle. Nevertheless, the curve could be recorded cleanly and the period time could be determined normally, because the amplitude did not play a role in the evaluation. As expected, the period times had only small deviations for the different currents. The damping coefficients were also plausible, as the damping coefficient increased exponentially as the current increased.
Furthermore, the dimensioning of the inertia of the three rods also worked. But the aluminum rod seemed to have too little inertia, as its period time was similar to that of the pendulum without a rod. As a result, no pendulum inertia could be determined depending on the aluminum rod. The two inertia obtained differ from each other and the error range of the two do not cover either. This could also be due to the inaccurate reading of the period time. Nevertheless, the order of magnitude seems to be correct.
Another unnoticed cause of the error could be the wear and aging of the setup, as the wire, for example, looked quite sensitive and worn out.
It can then be clearly stated that the REALTERM program should be revised and that several, heavier and longer rods should be used to better determine the unknown pendulum inertia.

List of Figures

List of Tables

List of Symbols

ω_0	Angular frequency
τ	
I	
I_S	
m	
d	
N	
A	
B	
t	
U_{ind}	
l	
ε_0	
ε_r	
C	
D	
ρ	
M	
φ	
R	
J	
k	
δ	
λ	
ω_d	
D^*	
$\vec{M_{Inert}}$	
$\vec{M_{Frict}}$	
$\vec{M_{Rest}}$	
$\vec{M_{Inert}}$	
$\hat{\varphi}$	
T_P	
J_P	
J_R	
J_Z	
r	
x	
L	
U_C	
U_0	
U_{th}	
Δt_{th}	
χ	
χ'	
C_{max}	
n	
s	
o	
I_c	
T	
δ_e	
δ_p	
m_{Ri}	
Ω_{Ri}	
l_{Ri}	
J_{R1}	

A Appendix

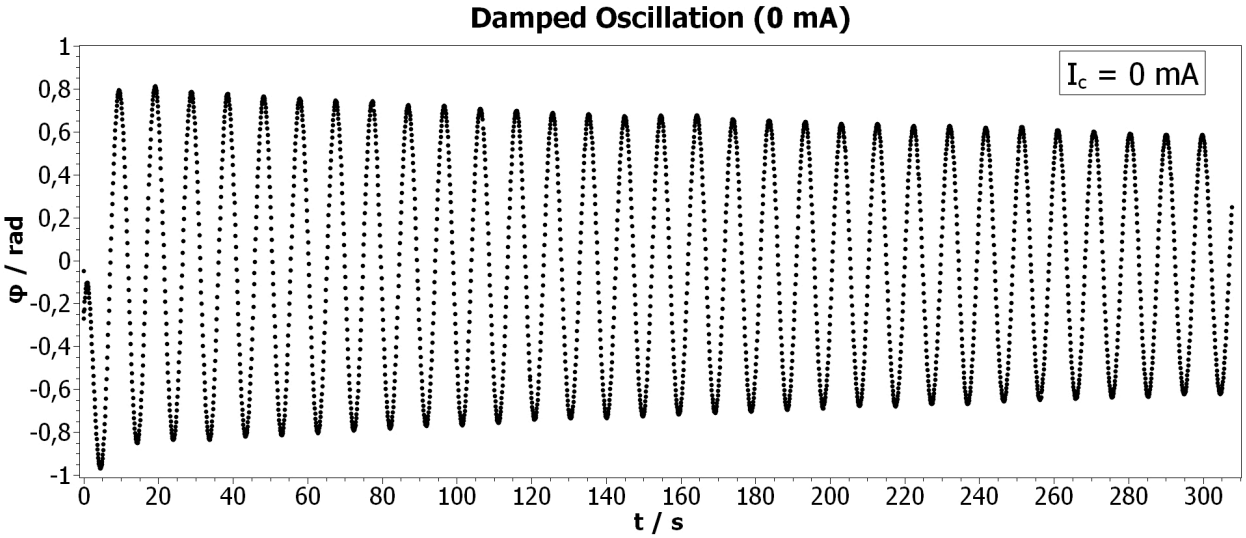

(a) $I_c = 0\,\mathrm{mA}$

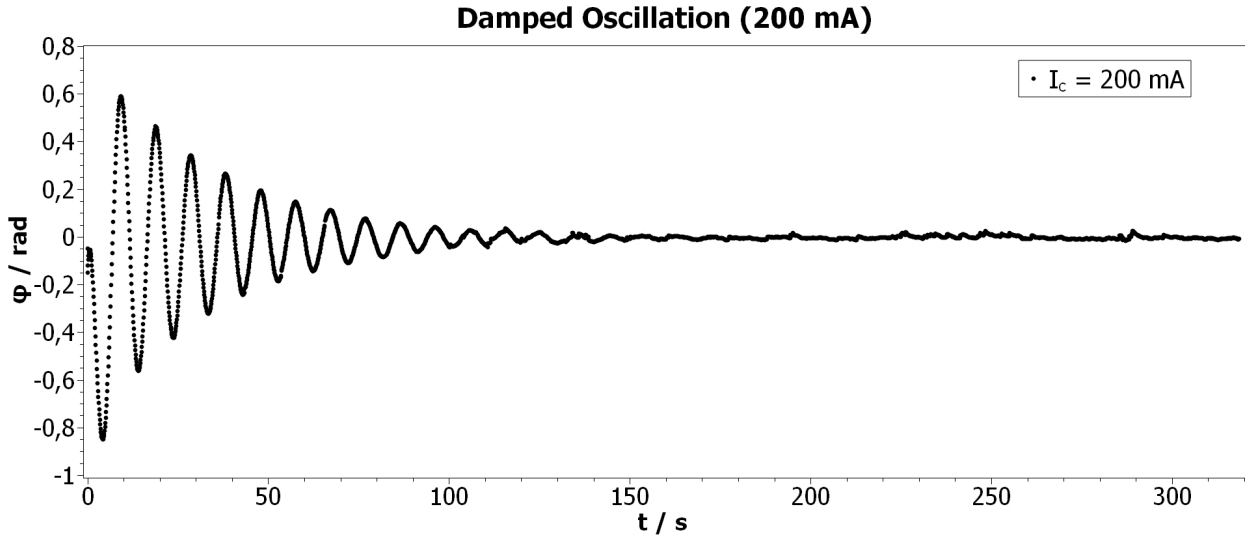

(b) $I_c = 200\,\mathrm{mA}$

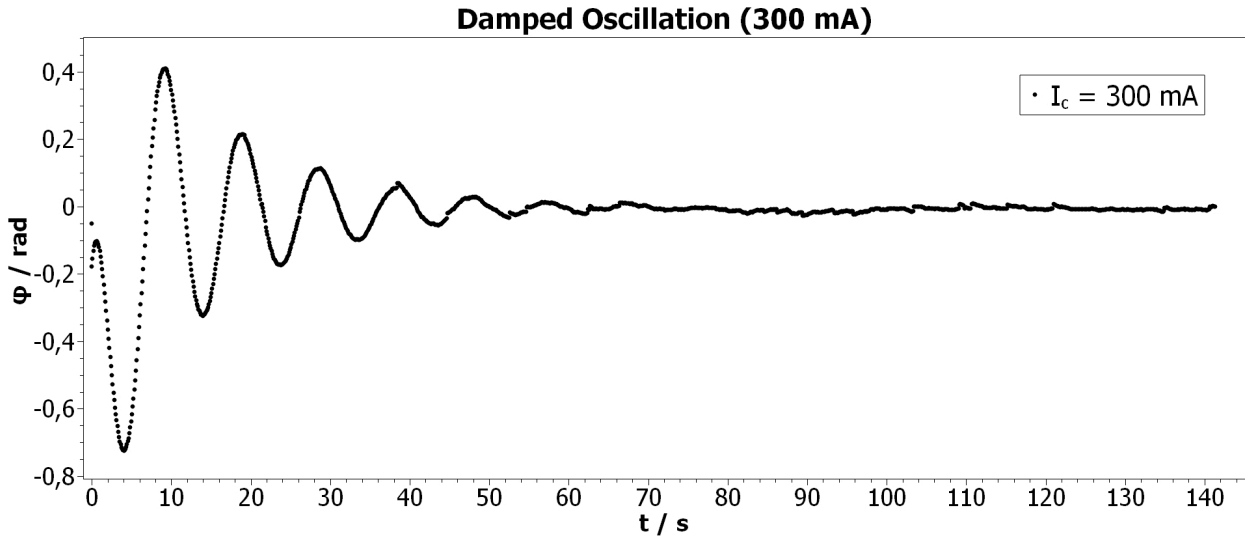

(c) $I_c = 300\,\mathrm{mA}$

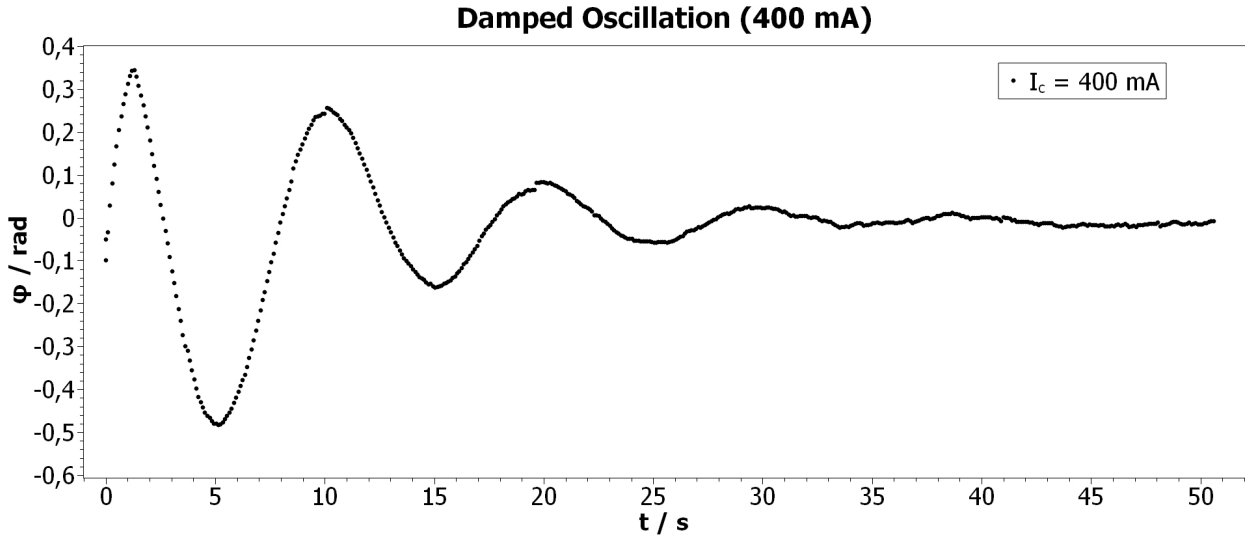

(d) $I_c = 400\,\mathrm{mA}$

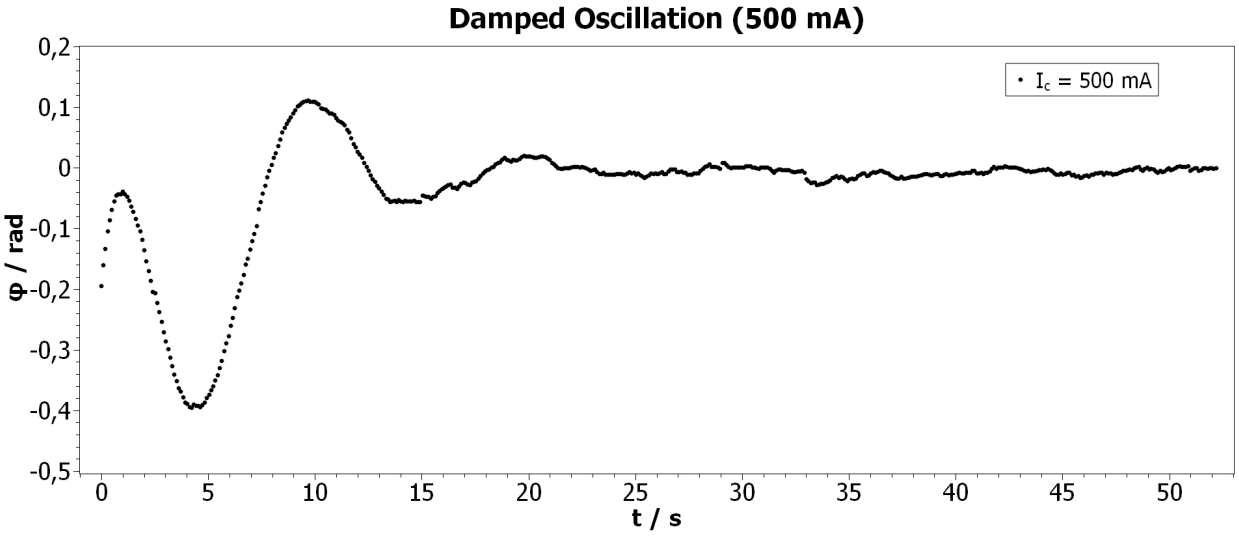

(e) $I_c = 500\,\mathrm{mA}$

Figure A.0: Plots of the tick rates over time with coil currents ranging from $0\,\mathrm{mA}$ to $500\,\mathrm{mA}$ in increments of $100\,\mathrm{mA}$

Bibliography

[1] Eichler, Hans-Joachim, Kronfeldt, Heinz-Detlef, and Sahm, Jürgen. *Das neue Physikalische Grundpraktikum*. ger. 3., ergänzte und aktualisierte Auflage 2016. Springer-Lehrbuch. Eichler, Hans-Joachim (VerfasserIn) Kronfeldt, Heinz-Detlef (VerfasserIn) Sahm, Jürgen (VerfasserIn). Berlin and Heidelberg: Springer Spektrum, 2016. 470 pp. ISBN: 978-3-662-49022-8. DOI: 10.1007/978-3-662-49023-5.